

Supporting Information

Synthesis, functionalisation and post-synthetic modification of bismuth metal-organic frameworks

M. Köppen,^a O. Beyer,^b S. Wuttke,^c U. Lüning,^{b,*} and N. Stock^{a,*}

^aInstitut für Anorganische Chemie, Christian-Albrechts-Universität zu Kiel, Max-Eyth-Str. 2, 24118 Kiel, Germany

^bOtto Diels-Institut für Organische Chemie, Christian-Albrechts-Universität zu Kiel, Otto-Hahn-Platz 4, 24118 Kiel, Germany

^cDepartment of Chemistry and Center for NanoScience (CeNS), LMU München, Butenandtstraße 11, 81377 München, Germany

* correspondence to:

stock@ac.uni-kiel.de

luening@oc.uni-kiel.de

Table of contents

Organic linker synthesis	4
Synthesis of H ₃ TATB	4
Synthesis of H ₃ TATB-NH ₂	4
CAU-7-TATB [Bi(TATB)].....	6
LeBail fit and Rietveld refinement.....	6
Refinement details	6
LeBail plot of CAU-7-TATB (<i>as</i>)	7
PXRD patterns of CAU-7-TATB (<i>as</i>) and CAU-7-TATB (<i>ht</i>)	7
Rietveld plot of CAU-7-TATB (<i>ht</i>).....	8
Selected bond lengths	9
Structure of CAU-7-TATB (<i>ht</i>)	10
Characterisation of CAU-7-TATB	12
Sorption.....	12
Infrared spectroscopy	13
Thermogravimetric and elemental analysis	13
CAU-7-TATB-NH ₂ [Bi(TATB-NH ₂)].....	15
LeBail fit.....	15
LeBail plot.....	15
Characterisation of CAU-7-TATB-NH ₂	16
Sorption.....	16
Scanning Electron Microscopy	18
Infrared spectroscopy, thermogravimetric and elemental analysis.....	19
CAU-35 [Bi ₂ (O)(OH)(TATB)]·H ₂ O	20
Structure solution and Rietveld refinement of CAU-35	20
Refinement details	20
Rietveld plot	21
Selected bond lengths	22
Structure of CAU-35	23
Characterisation of CAU-35.....	26
Sorption.....	26
Infrared spectroscopy	27
Thermogravimetric and elemental analysis	28

Post-synthetic modification	29
¹ H-NMR spectra.....	29
CAU-7-TATB-NH ₂ -AA.....	30
CAU-7-TATB-NH ₂ -VA.....	30
CAU-7-TATB-NH ₂ -SA	31
CAU-7-TATB-NH ₂ -PA.....	31
CAU-7-TATB-NH ₂ -PS	32
Comparison of PSM with valeric anhydride for two batches with different BET surface	32
X-ray powder diffraction	34
Sorption.....	35
Infrared spectroscopy	36
Thermogravimetric and elemental analysis	36
References	38

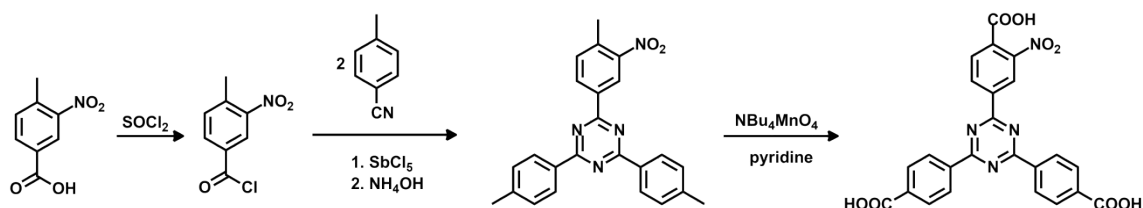
Organic linker synthesis

Synthesis of H₃TATB

The precursor 2,4,6-tris(4-methylphenyl)-1,3,5-triazine was synthesised by trimerization of 4-methylbenzonitrile. H₃TATB was obtained by oxidation of the methyl groups according to a literature procedure.¹

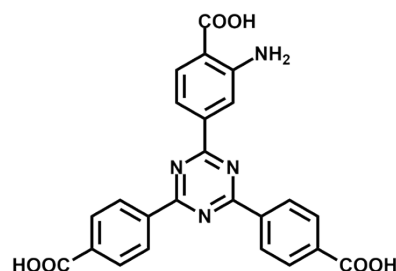
Synthesis of H₃TATB-NH₂

H₃TATB-NO₂ was synthesized according to the literature procedure by Mühlbauer et al.²



Reduction of the nitro group gave H₃TATB-NH₂ by using the following procedure:

2-(4-Carboxy-3-nitrophenyl)-4,6-bis(4-carboxyphenyl)-1,3,5-triazine (H₃TATB-NO₂, 2.50 g, 5.14 mmol) and potassium carbonate (4.47 g, 25.7 mmol) were suspended in water (80 mL) and stirred until the entire solid was dissolved. Ethanol (30 mL) was added to the solution followed by sodium dithionite (3.55 g, 25.7 mmol). The reaction mixture was stirred for 1 h at room temperature. Ethanol was removed under reduced pressure and the residue was poured into conc. hydrochloric acid (200 mL). The precipitate was filtered off and the residue was washed thoroughly with water. The resulting solid was recrystallized from DMSO/water to yield 1.72 g (3.77 mmol, 73 %) of a yellow solid.



M. p.: >300 °C

¹H-NMR (500 MHz, DMSO-*d*₆): δ = 8.82 (d, ³J = 8.6 Hz, 4H, Ar'-*H*-2,6), 8.23 (d, ⁴J = 1.6 Hz, 1H, Ar-*H*-2), 8.20 (d, ³J = 8.6 Hz, 4H, Ar'-*H*-3,5), 7.94 (d, ³J = 8.3 Hz, 1H, Ar-*H*-5), 7.83 (dd, ³J = 8.3 Hz, ⁴J = 1.6 Hz, 1H, Ar-*H*-6) ppm.

¹³C-NMR (125 MHz, DMSO-*d*₆): δ = 171.1 (s, Tri-C-2), 170.5 (s, Tri-C-4,6), 169.2 (s, Ar-CO₂H), 166.8 (s, Ar'-CO₂H), 151.6 (s, Ar-C-3), 139.4 (s, Ar-C-1), 139.0 (s, Ar'-C-1), 134.7 (s, Ar'-C-4), 131.8 (d, Ar-C-5), 129.8 (d, Ar'-C-3,5), 128.8 (d, Ar'-C-2,6), 117.1 (d, Ar-C-2), 114.3 (d, Ar-C-6), 113.0 (s, Ar-C-4) ppm.

IR (ATR): $\tilde{\nu}$ = 2982 (br., OH), 1685 (C=O), 1579, 1505 (arom. C=C, arom. C=N), 1358 (C-N), 766 (1,4-disubst. aryl, 1,2,4-trisubst. aryl) cm⁻¹.

HRMS (EI): *m/z* = C₂₄H₁₆N₄O₆ calcd. 456.1069; meas. 456.1056 (Δ 2.9 ppm).

EA: $C_{24}H_{16}N_4O_6$ (456.41): calcd. C 63.16 H 3.53 N 12.28;

$C_{24}H_{16}N_4O_6 \cdot 1.5 H_2O$ (483.43): calcd. C 59.63 H 3.96 N 11.59;

meas. C 59.48 H 3.95 N 11.68.

CAU-7-TATB [Bi(TATB)]

LeBail fit and Rietveld refinement

Refinement details

The Rietveld refinement was performed with TOPAS Academic 4.1³ using one individual bismuth atom and one linker molecule as rigid body with z-matrix. Torsion angles of phenyl rings and carboxylate oxygen atoms were refined individually, bond lengths in groups ($C_{\text{triazine}}-N_{\text{triazine}}, C_{\text{phenyl}}-C_{\text{phenyl}}$).

Table S1: Cell parameters of CAU-7 (from Rietveld refinement),⁴ of CAU-7-TATB (*as*, from LeBail fit) and of CAU-7-TATB (*ht*, from Rietveld refinement).

	CAU-7	CAU-7-TATB (<i>as</i>)	CAU-7-TATB (<i>ht</i>)
Space group	<i>Pb2₁a</i>	<i>Pc</i> (one poss.)	<i>Pb2₁a</i>
<i>a</i>	32.36(1) Å	27.357(3) Å	31.001(6) Å
<i>b</i>	28.084(7) Å	4.4766(6) Å	27.623(5) Å
<i>c</i>	3.9132(9) Å	30.598(3) Å	3.913(1) Å
α	90°	90°	90°
β	90°	90.910(5)°	90°
γ	90°	90°	90°
R_{wp}	9.43	4.269	3.303
GOF	2.85	1.463	5.371

LeBail plot of CAU-7-TATB (*as*)

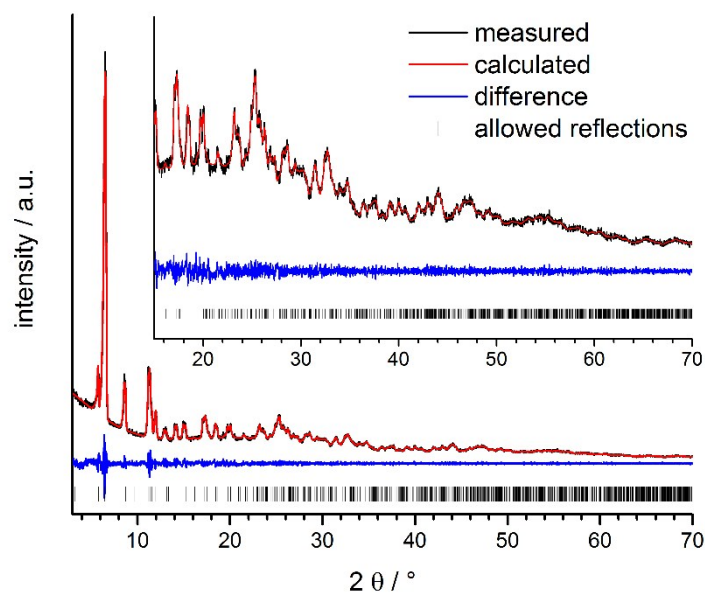


Figure S1: LeBail plot of the refinement of CAU-7-TATB (*as*). Measured and calculated PXRD data, the difference of both and the allowed reflections are shown in black, red, blue and as black bars, respectively.

PXRD patterns of CAU-7-TATB (*as*) and CAU-7-TATB (*ht*)

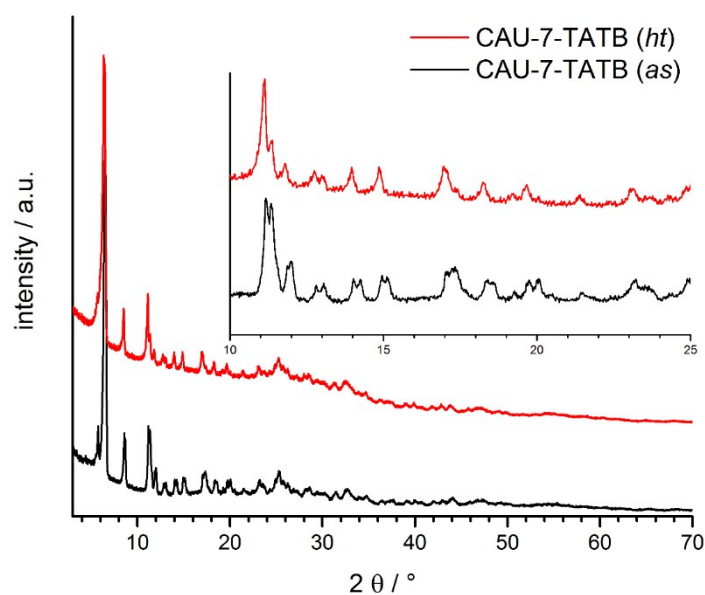


Figure S2: PXRD patterns of CAU-7-TATB (*as*) and CAU-7-TATB (*ht*) in comparison.

Rietveld plot of CAU-7-TATB (*ht*)

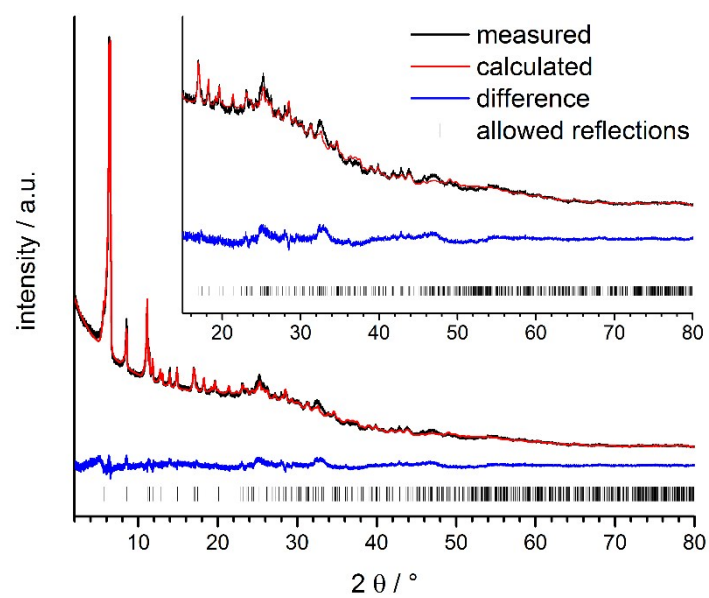


Figure S3: Rietveld plot of the refinement of CAU-7-TATB (*ht*). Measured and calculated PXRD data, the difference of both and the allowed reflections are shown in black, red, blue and as black bars, respectively.

Selected bond lengths

Table S2: Selected bond lengths in CAU-7-TATB (*ht*).

Atom 1	Symmetry 1	Atom 2	Symmetry 2	Distance / Å
Bi1	x, y, z	O1	x, y, -1+z	2.465(17)
Bi1	x, y, z	O2	x, y, z	2.762(11)
Bi1	x, y, z	O2	x, y, -1+z	2.690(11)
Bi1	x, y, z	O3	0.5+x, y, 1-z	2.982(10)
Bi1	x, y, z	O3	0.5+x, y, -z	2.444(10)
Bi1	x, y, z	O4	0.5+x, y, 1-z	2.489(14)
Bi1	x, y, z	O4	0.5+x, y, -z	2.487(14)
Bi1	x, y, z	O5	1.5-x, 0.5+y, z	2.881(14)
Bi1	x, y, z	O5	1.5-x, 0.5+y, -1+z	2.231(16)
Bi1	x, y, z	O6	1.5-x, 0.5+y, -1+z	2.678(14)
C1/C9/C17		C2/C10/C18		1.4064(2)
C5/C13/C21		C8/C16/C24		1.4064(2)
N		C		1.4474(2)
C (phenyl)		C (phenyl)		1.4474(2)

Structure of CAU-7-TATB (*ht*)

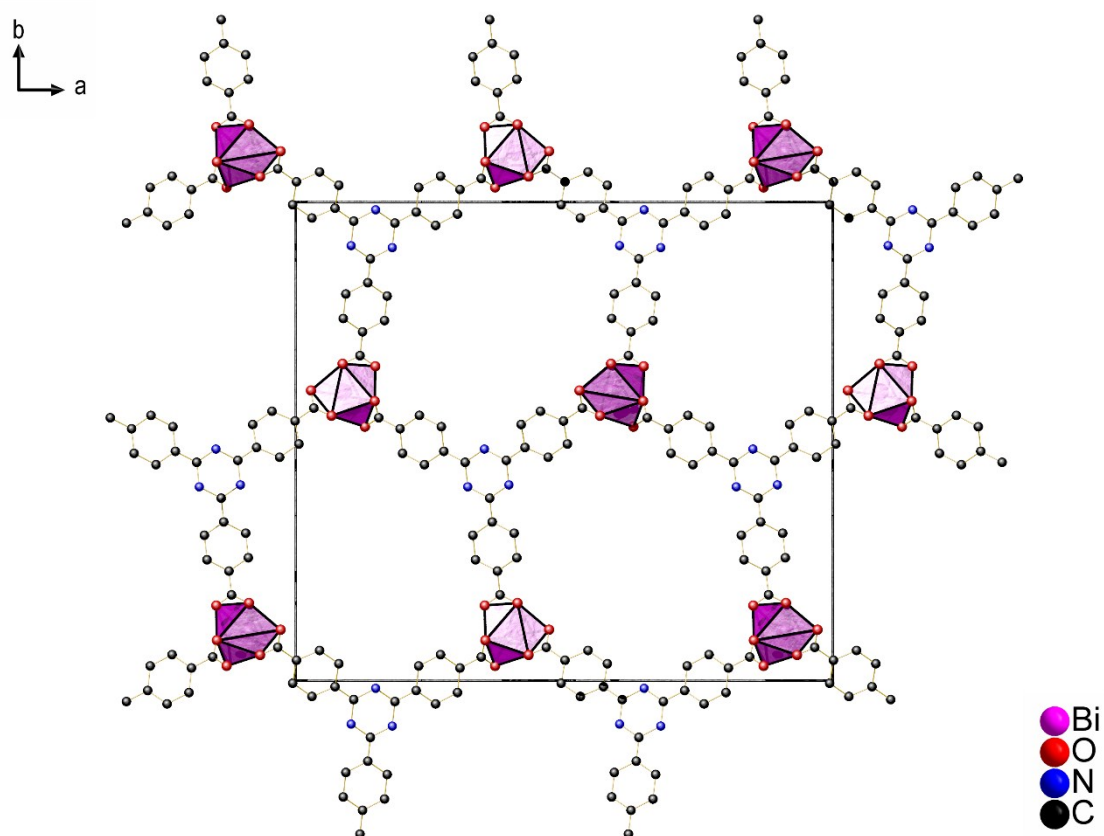


Figure S4: Crystal structure of CAU-7-TATB (*ht*), view along [001]. The unit cell dimension is represented by the box.

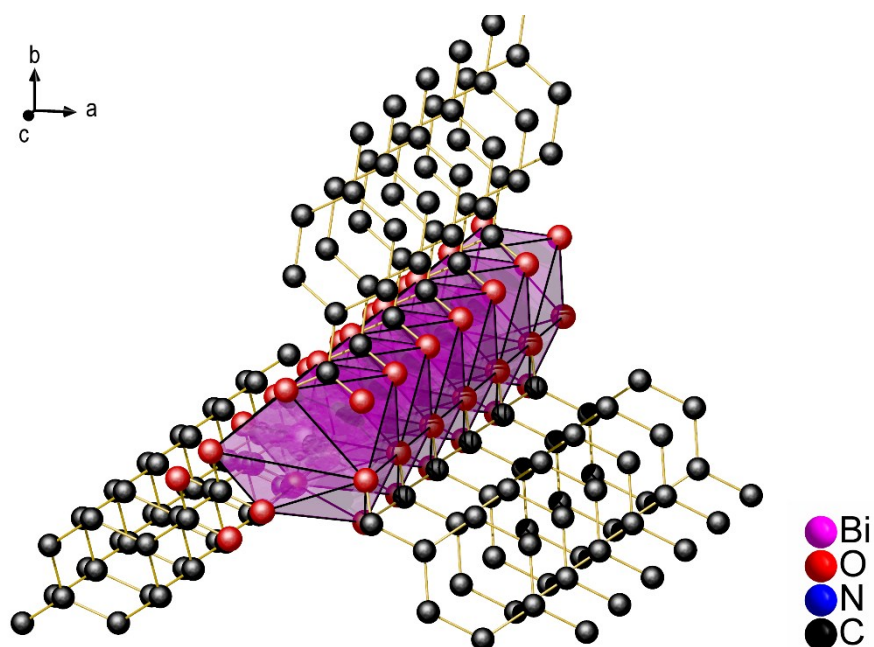


Figure S5: Linear chain in crystal structure of CAU-7-TATB (*ht*). See also Fig. S22.

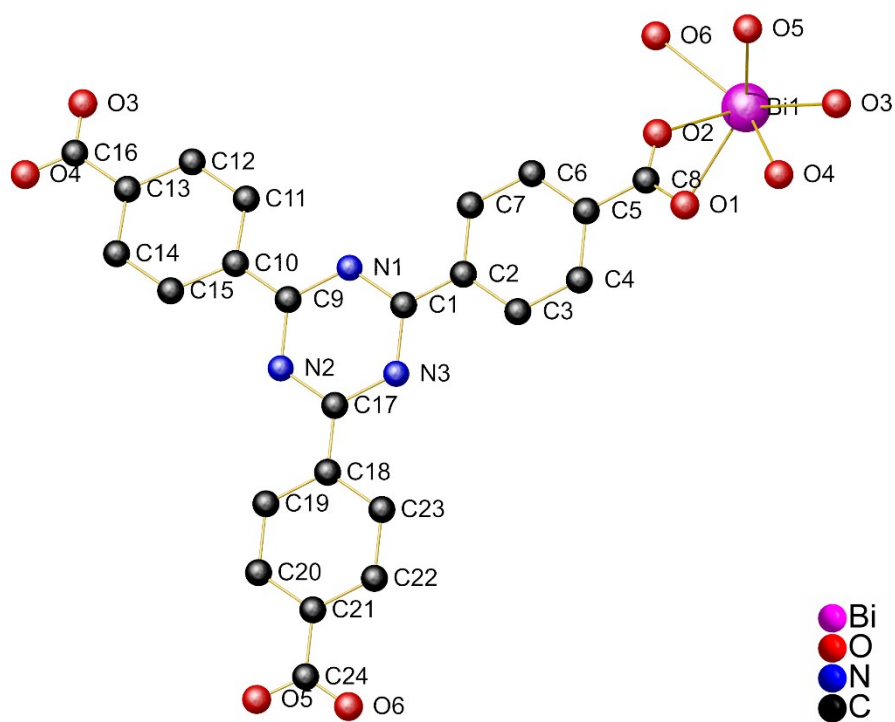


Figure S6: Extended asymmetric unit of the crystal structure of CAU-7-TATB (*ht*).

Characterisation of CAU-7-TATB

Sorption

The N₂ sorption measurement leads to a specific BET surface area of $A_{\text{BET}} = 813 \text{ m}^2/\text{g}$ and a micropore volume of $V_{\text{mic}} = 0.31 \text{ cm}^3/\text{g}$. These values correlate well with the theoretical maximum values of $A_{\text{BET,theo}} = 867 \text{ m}^2/\text{g}$ and $V_{\text{mic,theo}} = 0.32 \text{ cm}^3/\text{g}$, calculated with accessible solvent surface module in Materials Studio 5.5 using a probe molecule radius of 1.82 Å for simulated N₂.^{5,6}

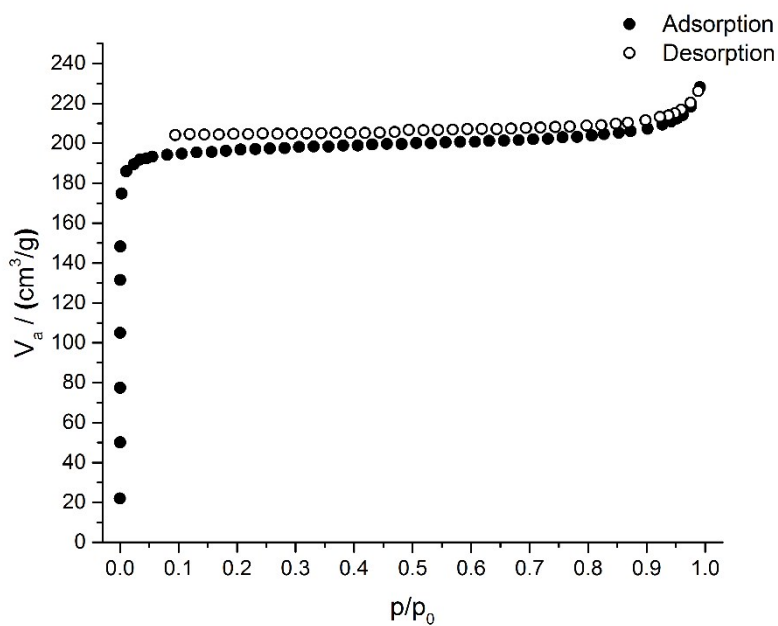


Figure S7: N₂ sorption isotherm of CAU-7-TATB (*ht*), measured at 77 K. Activation of the sample at 150 °C for 12 h in vacuum.

Infrared spectroscopy

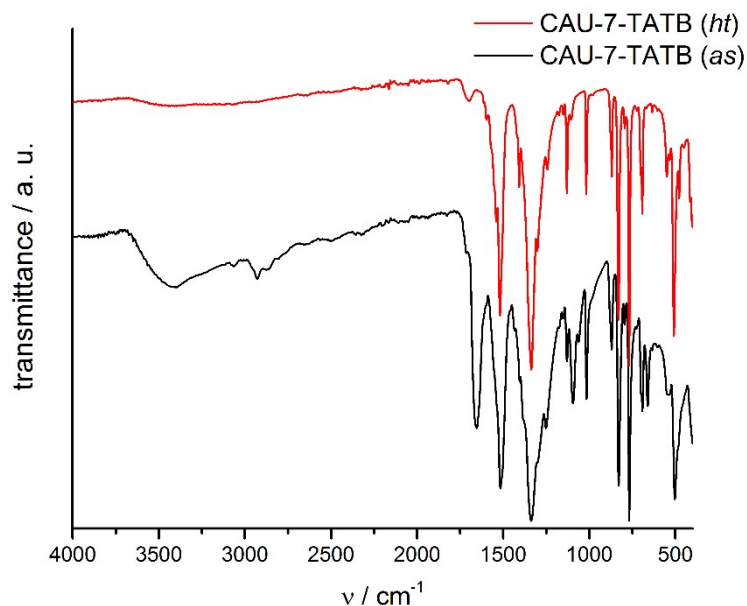


Figure S8: IR spectra of CAU-7-TATB. Characteristic frequencies: 1518 cm^{-1} (asymm. carboxylate), 1410-1240 cm^{-1} (symm. carboxylate), 1017 cm^{-1} , 880-692 cm^{-1} (aryl-H). The only significant differences for CAU-7-TATB (*as*) are the bands at 3700-2150 cm^{-1} (OH, water) and all bands that are attributed to DMF molecules inside the pores (2927 cm^{-1} , 2871 cm^{-1} , 1654 cm^{-1}).

Thermogravimetric and elemental analysis

The chemical formulas of the *as*- and *ht*-phase were determined by combining the results from TG and elemental analyses and are summarized in the following table. The results of the thermogravimetric analysis are in agreement with the theoretical weight losses (meas.: 19.5 %, 50.7 %; theo.: 21.9 %, 50.0 %; first step: pore content, second step: decomposition of the framework). TG and elemental analyses were performed under ambient conditions, which might have led to water adsorption from the air.

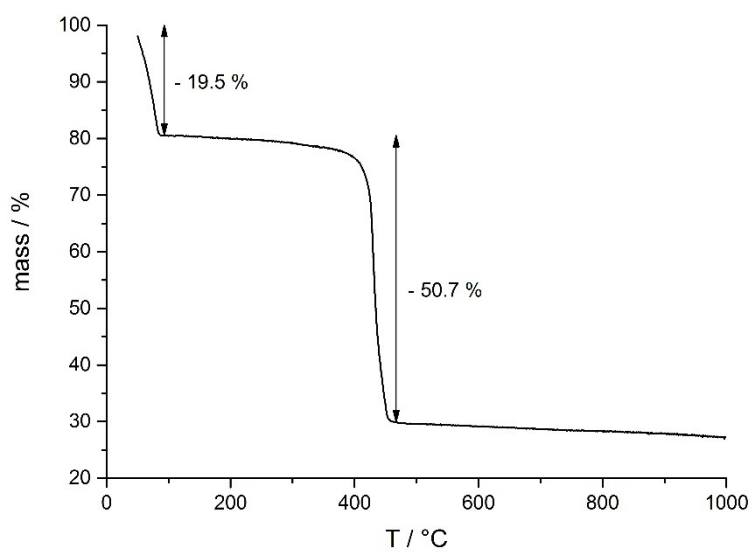


Figure S9: Thermogravimetric analysis of CAU-7-TATB (*ht*).

Table S3: Results of the elemental analyses of CAU-7-TATB (*as*, top) and CAU-7-TATB (*ht*, bottom).

Chemical formula		C / %	H / %	N / %	S / %
[Bi(TATB)]·DMF·6H ₂ O	meas.	37.29	2.93	7.84	0.00
	theo.	39.14	3.77	6.76	0.00
[Bi(TATB)]·9H ₂ O	meas.	35.96	1.52	5.57	0.00
	theo.	35.61	3.74	5.19	0.00

CAU-7-TATB-NH₂ [Bi(TATB-NH₂)]

LeBail fit

Table S4: Results of the LeBail fit of [Bi(TATB-NH₂)].

CAU-7-TATB-NH ₂	
Space group	<i>Pb2₁a</i>
<i>a</i>	30.861(3) Å
<i>b</i>	27.521(2) Å
<i>b</i>	3.8907(5) Å
α	90°
β	90°
γ	90°
R _{wp}	3.32
GOF	1.72

LeBail plot

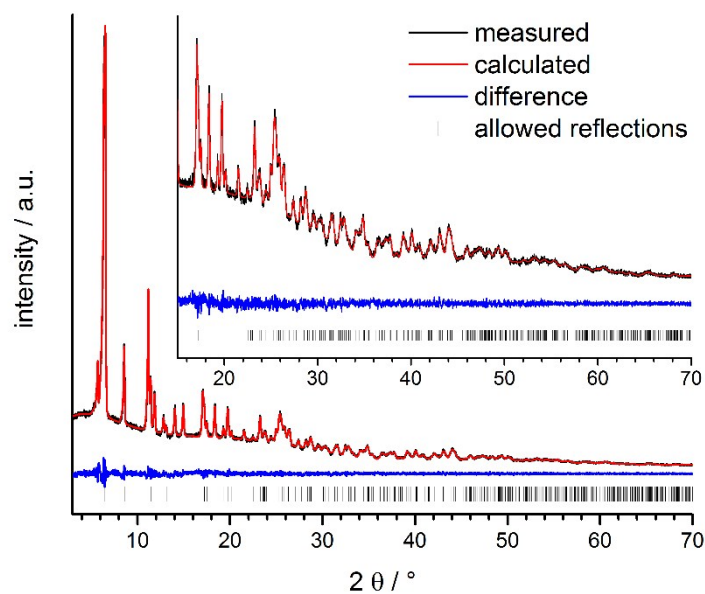


Figure S10: LeBail plot of the refinement of CAU-7-TATB-NH₂. Measured and calculated PXRD data, the difference of both and the allowed reflections are shown in black, red, blue and as black bars, respectively.

Characterisation of CAU-7-TATB-NH₂

Sorption

The N₂ sorption measurements of the CAU-7-TATB-NH₂ samples, obtained from different synthesis batches, vary strongly. Fig. S11 shows the adsorption curves of eight exemplary reaction products. The results of the BET analyses are summarized in the following table.

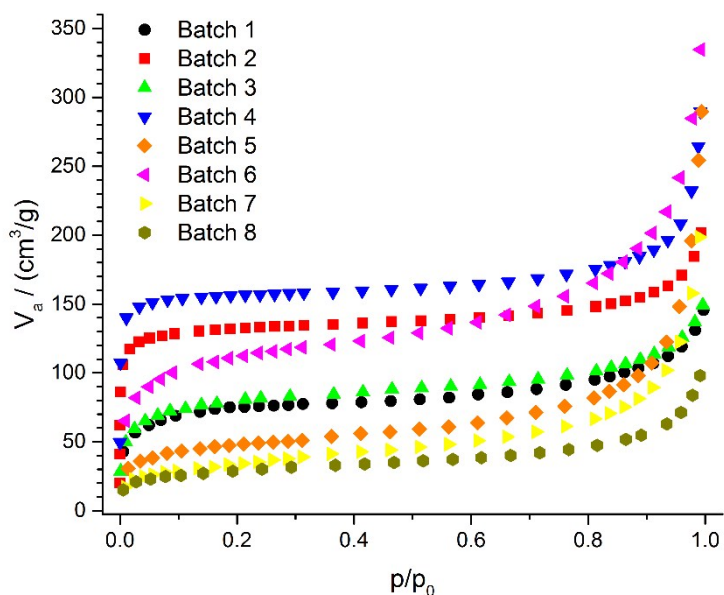


Figure S11: N₂ adsorption isotherms of eight different batches of CAU-7-TATB-NH₂, measured at 77 K. All batches were obtained under identical reaction conditions using the same batches of starting materials. Activation of the samples at 190 °C for 12 h in vacuum. Only the adsorption curves are shown for more clarity.

Table S5: Specific BET surface areas and micropore volumes of eight different batches of CAU-7-TATB-NH₂.

Sample	A _{BET} / (m ² /g)	V _{mic} / (cm ³ /g)
Batch 1	279	0.12
Batch 2	519	0.21
Batch 3	295	0.14
Batch 4	627	0.25
Batch 5	176	0.09
Batch 6	415	0.20
Batch 7	120	0.07
Batch 8	104	0.06

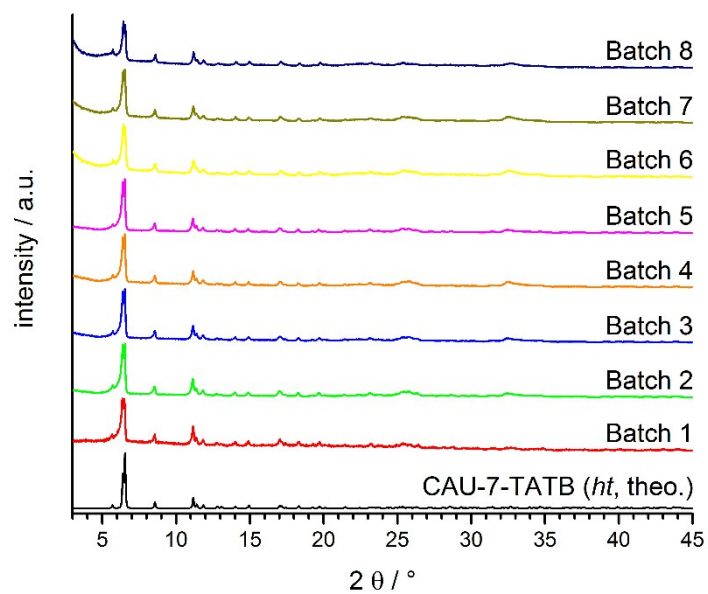


Figure S12: PXRD patterns of eight different batches of CAU-7-TATB-NH₂. For all patterns there is no significant difference in the PXRD patterns of these batches.

Scanning Electron Microscopy

The SEM experiments, which are presented here, were performed on a *Jeol JSM-6500F* with EDX-Detektor and *Inca*-software (*Oxford Instruments*). For sample preparation, an ethanolic dispersion of the MOF sample was dried and subsequently sputtered with carbon.

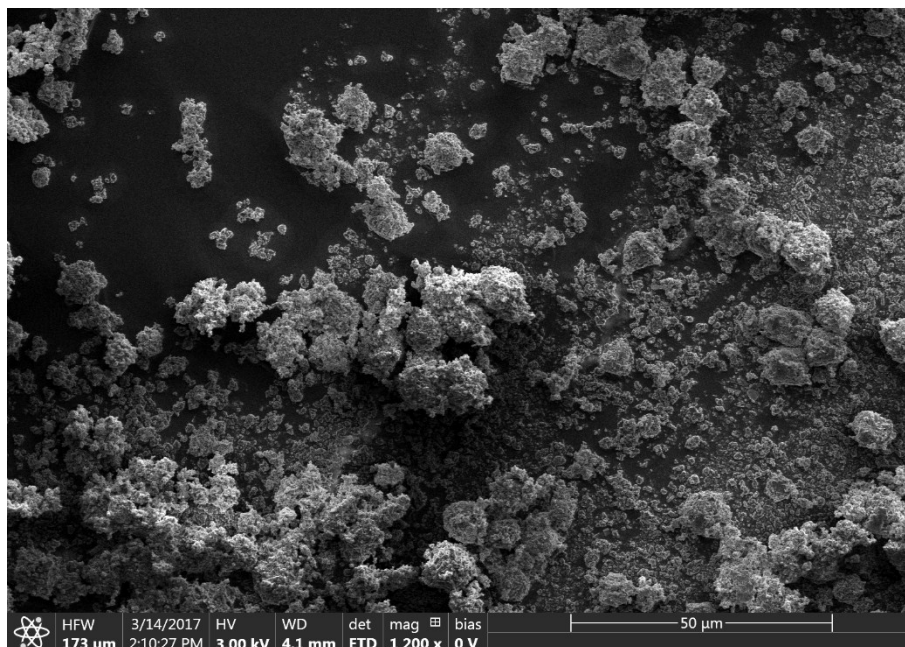


Figure S13: SEM micrograph of CAU-7-NH₂ with 50 µm scale bar (*Batch 8*, $A_{\text{BET}} = 104 \text{ m}^2/\text{g}$).

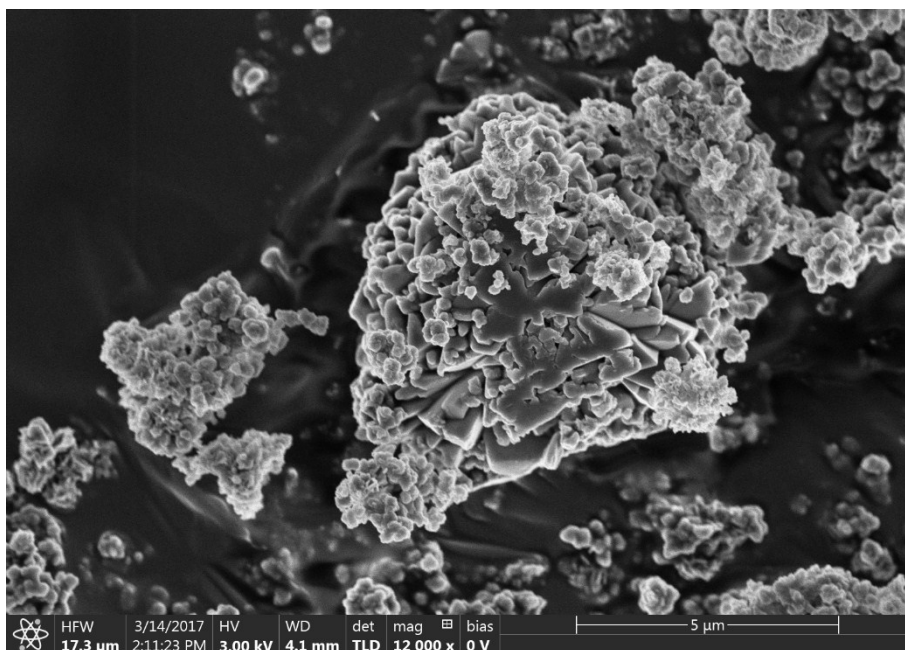


Figure S14: SEM micrograph of CAU-7-NH₂ with 5 µm scale bar (*Batch 8*, $A_{\text{BET}} = 104 \text{ m}^2/\text{g}$).

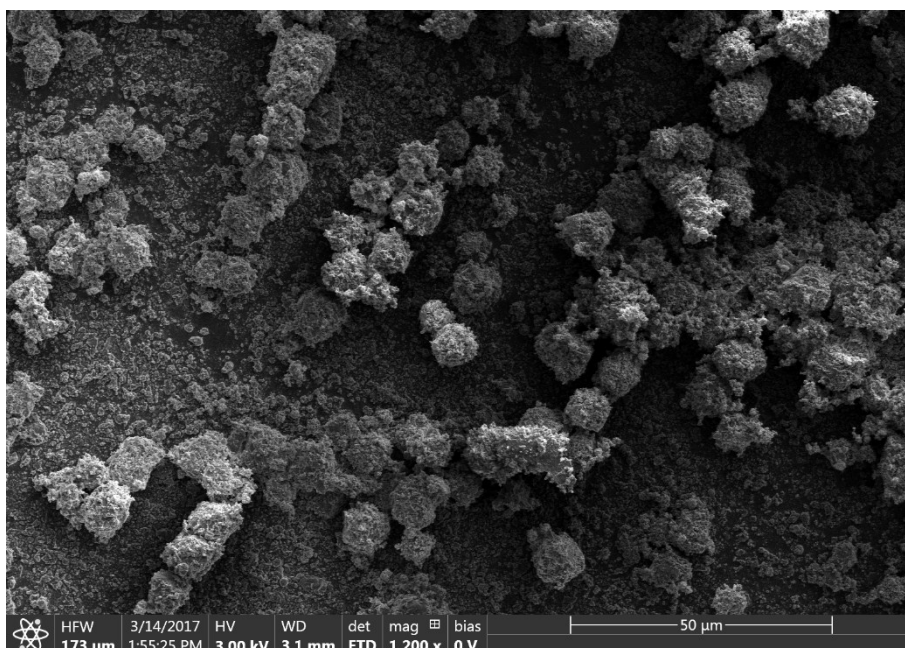


Figure S15: SEM micrograph of CAU-7-NH₂ with 50 µm scale bar (*Batch 4*, $A_{\text{BET}} = 627 \text{ m}^2/\text{g}$).

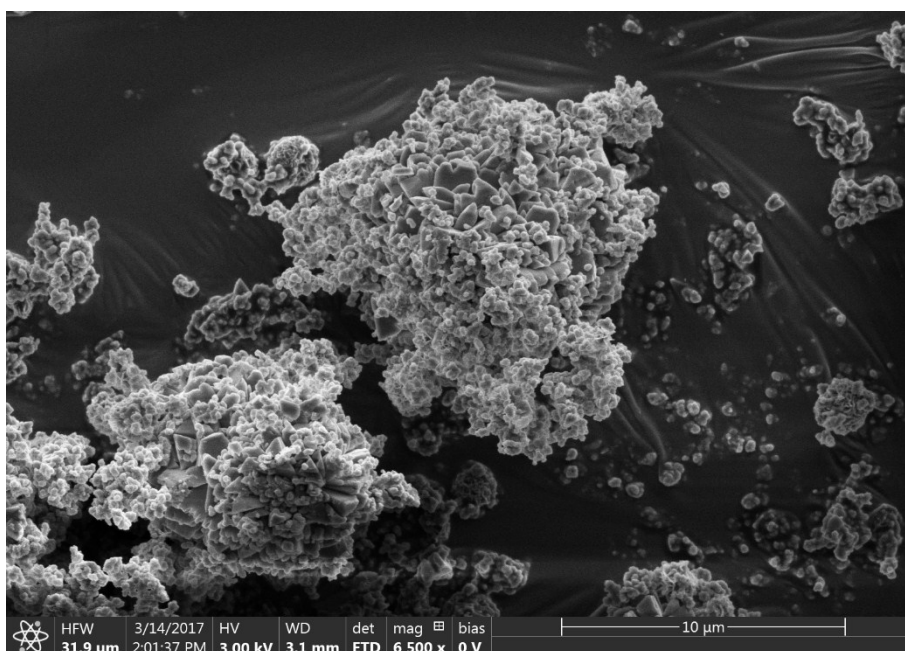


Figure S16: SEM micrograph of CAU-7-NH₂ with 5 µm scale bar (*Batch 4*, $A_{\text{BET}} = 627 \text{ m}^2/\text{g}$).

Infrared spectroscopy, thermogravimetric and elemental analysis

Further characterisation of CAU-7-TATB-NH₂ is summarized in the post-synthetic modification part of this document for better comparison.

CAU-35 [Bi₂(O)(OH)(TATB)]·H₂O

Structure solution and Rietveld refinement of CAU-35

Refinement details

After indexing the powder pattern with TOPAS Academic 4.1,³ the structure was solved using the software FOX,⁷ starting from two Bi atoms and one TATB³⁻ molecule, which was introduced as a rigid body. Bi-positions were located first and fixed afterwards, since bismuth is the most dominant scatterer in the structure. The *parallel tempering function* was used for the solution of the structure.

The Rietveld refinement was performed with TOPAS Academic 4.1³ using two individual bismuth atoms and one linker molecule as rigid body with z-matrix. Torsion angles of phenyl rings and carboxylate oxygen atoms were refined individually, bond lengths in groups (C_{triazine}-N_{triazine}, C_{phenyl}-C_{phenyl}, C_{carboxy}-O_{carboxy}). The two separate oxygen atoms in the inorganic building unit were added from Fourier difference analysis.

Table S6: Results of the structure refinement of [Bi₂(O)(OH)(TATB)]·H₂O.

	CAU-35
Space group	<i>Pna2</i> ₁
<i>a</i>	20.868(2) Å
<i>b</i>	31.658(3) Å
<i>b</i>	3.9596(3) Å
α	90°
β	90°
γ	90°
R _{wp}	4.94
GOF	1.74

Rietveld plot

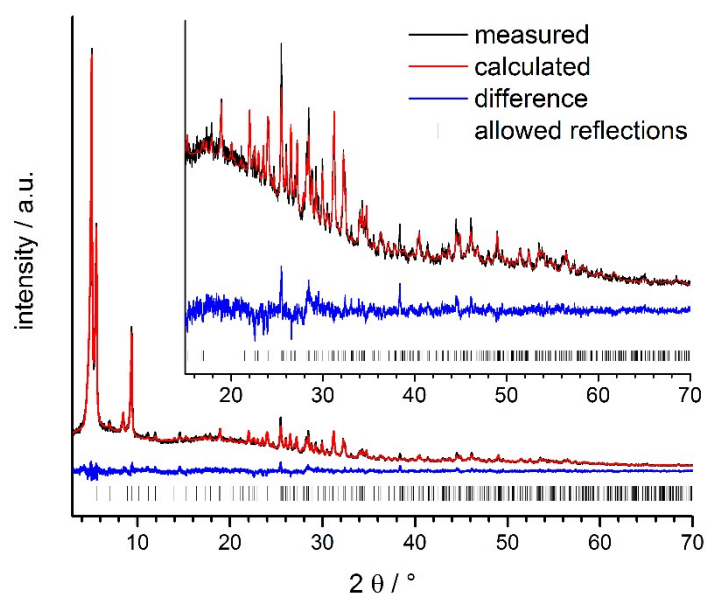


Figure S17: Rietveld plot of the refinement of CAU-35. Measured and calculated PXRD data, the difference of both and the allowed reflections are shown in black, red, blue and as black bars, respectively.

Selected bond lengths

Table S7: Selected bond lengths in CAU-35.

Atom 1	Symmetry 1	Atom 2	Symmetry 2	Distance / Å
Bi1	x, y, z	O7	0.5+x, 0.5-y, z	2.141(53)
Bi1	x, y, z	O3	1.5-x, 0.5+y, -0.5+z	2.287(12)
Bi1	x, y, z	O3	1.5-x, 0.5+y, -1.5+z	3.003(14)
Bi1	x, y, z	O7	1.5-x, -0.5+y, -0.5+z	2.53(48)
Bi1	x, y, z	O7	1.5-x, -0.5+y, 0.5+z	2.44(47)
Bi1	x, y, z	O8	1.5-x, -0.5+y, 0.5+z	2.115(52)
Bi1	x, y, z	O1	1-x, -y, -0.5+z	2.3236(97)
Bi2	x, y, z	O6	x, 1+y, z	2.455(12)
Bi2	x, y, z	O8	1.5-x, 0.5+y, 1.5+z	2.29(16)
Bi2	x, y, z	O8	1.5-x, 0.5+y, 0.5+z	2.36(16)
Bi2	x, y, z	O7	1.5-x, 0.5+y, 0.5+z	2.853(50)
Bi2	x, y, z	O2	1-x, 1-y, -0.5+z	2.1691(88)
Bi2	x, y, z	O5	x, 1+y, z	2.1706(87)
Bi2	x, y, z	O4	0.5+x, 0.5-y, -1+z	2.362(13)
C1/C2/C3		C4/C11/C18		1.3175(1)
C7/C14/C21		C10/C17/C24		1.4926(1)
N		C		1.3500(1)
C (phenyl)		C (phenyl)		1.3809(1)

Structure of CAU-35

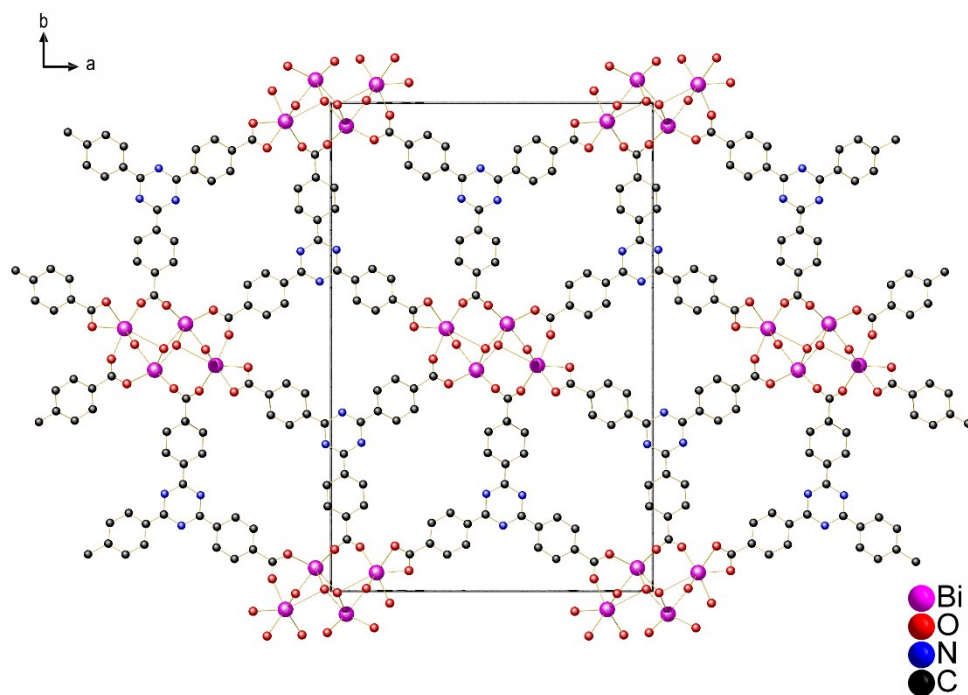


Figure S18: Crystal structure of CAU-35, view along [001]. The unit cell dimension is represented by the box.

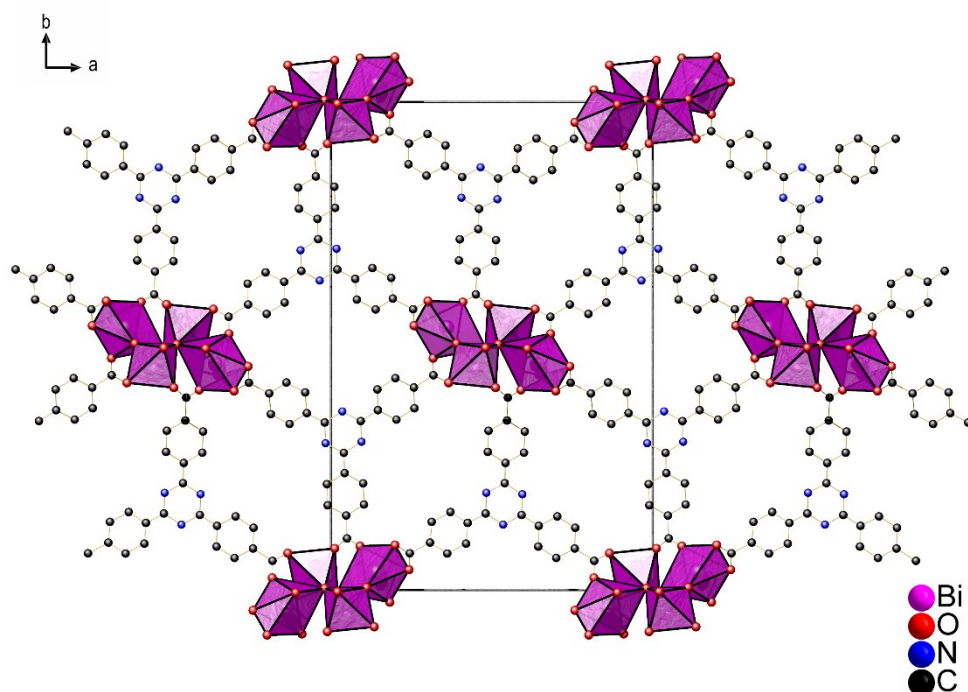


Figure S19: Crystal structure of CAU-35, view along [001]. The unit cell dimension is represented by the box.

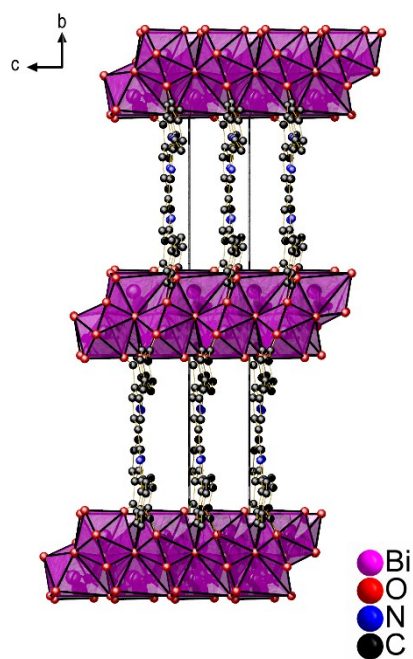


Figure S20: Crystal structure of CAU-35, view along [100]. The unit cell dimension is represented by the box.

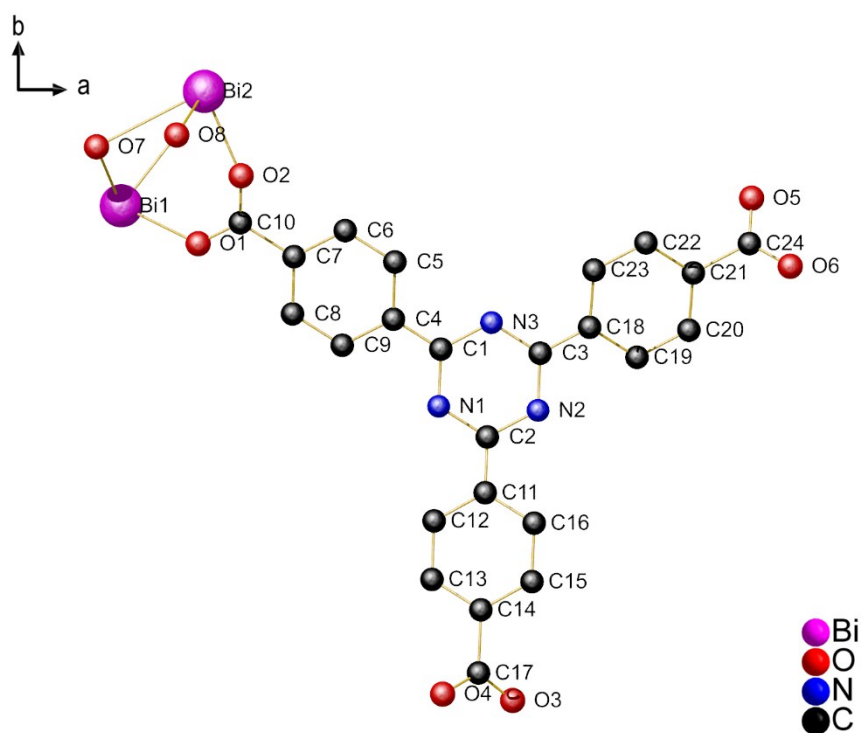


Figure S21: Asymmetric unit of the crystal structure of CAU-35.

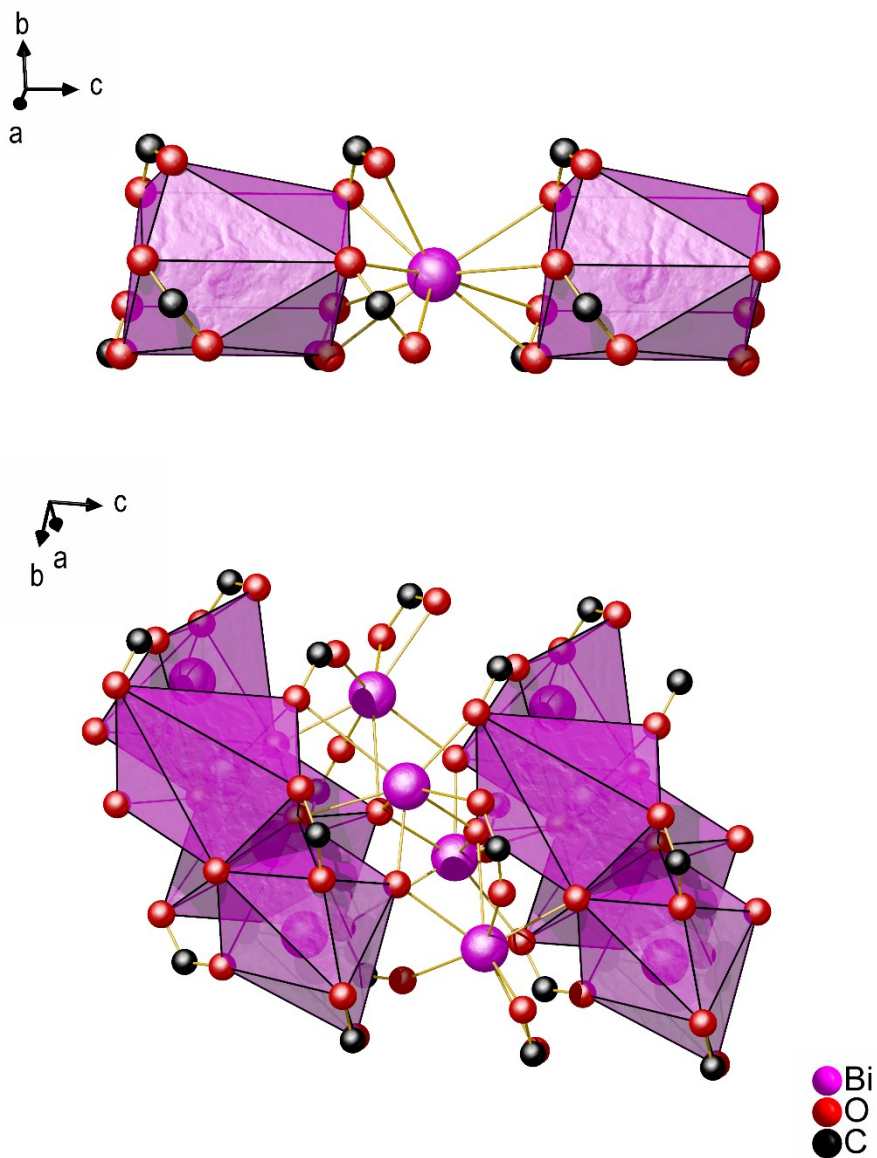


Figure S22: IBUs in CAU-7-TATB and CAU-35, on top and bottom, respectively.

Characterisation of CAU-35

Sorption

The N₂ sorption measurement leads to a specific BET surface area of $A_{\text{BET}} = 77 \text{ m}^2/\text{g}$ and a micropore volume of $V_{\text{mic}} = 0.05 \text{ cm}^3/\text{g}$. This value correlates well with the theoretical maximum value of $V_{\text{mic,theo}} = 0.06 \text{ cm}^3/\text{g}$, calculated with accessible solvent surface module in Materials Studio 5.5 using a probe molecule radius of 1.82 \AA for simulated N₂.^{5,6}

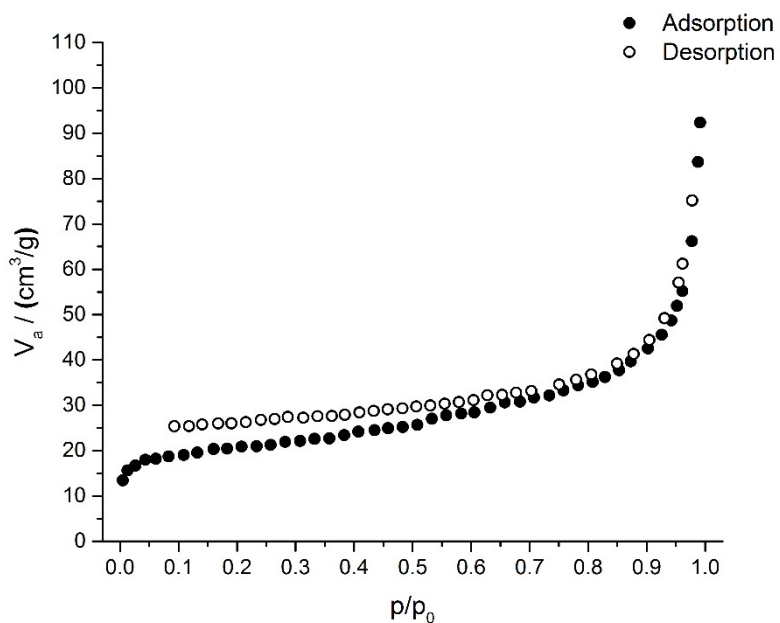


Figure S23: N₂ sorption isotherm of CAU-35, measured at 77 K. Activation of the sample at 150 °C for 12 h in vacuum.

Infrared spectroscopy

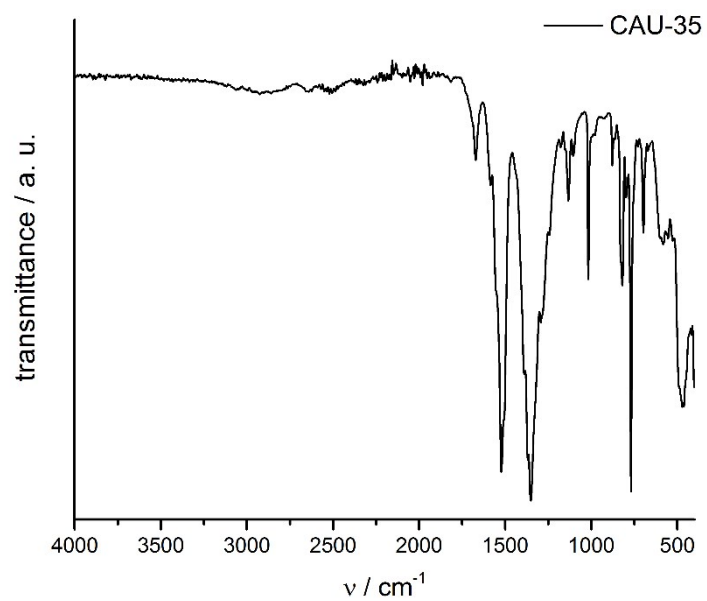


Figure S24: IR spectrum of CAU-35. Characteristic frequencies: 1671 cm^{-1} , 1585 cm^{-1} (C-N, triazine), 1522 cm^{-1} (asymm. carboxylate), 1351 cm^{-1} (symm. carboxylate), 1018 cm^{-1} , 820-697 cm^{-1} (aryl-H).

Thermogravimetric and elemental analysis

The chemical formula of CAU-35 was also determined by combining TG and elemental analysis and is shown in the following table. The results of the thermogravimetric analysis agree reasonably well with this data (meas.: 2.6 %, 41.4 %; theo.: 2.0 %, 45.8 %; first step: pore content, second step: decomposition of the framework). TG and elemental analyses were performed under ambient conditions, which might have led to water adsorption from the air.

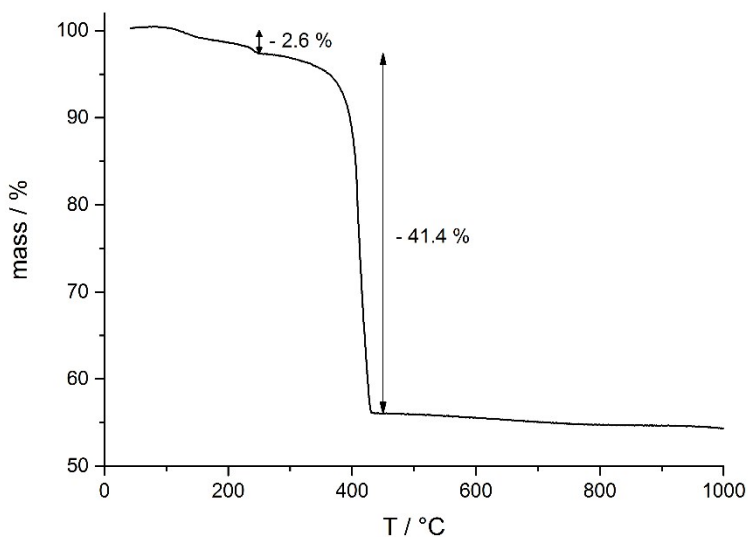


Figure S25: Thermogravimetric analysis of CAU-35.

Table S8: Results of the elemental analysis of CAU-35.

Chemical formula		C / %	H / %	N / %	S / %
[Bi ₂ (O)(OH)(TATB)]·H ₂ O	meas.	32.77	1.41	4.97	0.00
	theo.	31.77	1.67	4.63	0.00

Post-synthetic modification

For the characterisation of CAU-7-TATB-NH₂ and the five products of the PSM reactions, eight synthesis batches of CAU-7-TATB-NH₂ were combined and mixed. All PSM reactions and characterisations were performed with this mixture to facilitate the highest data consistence.

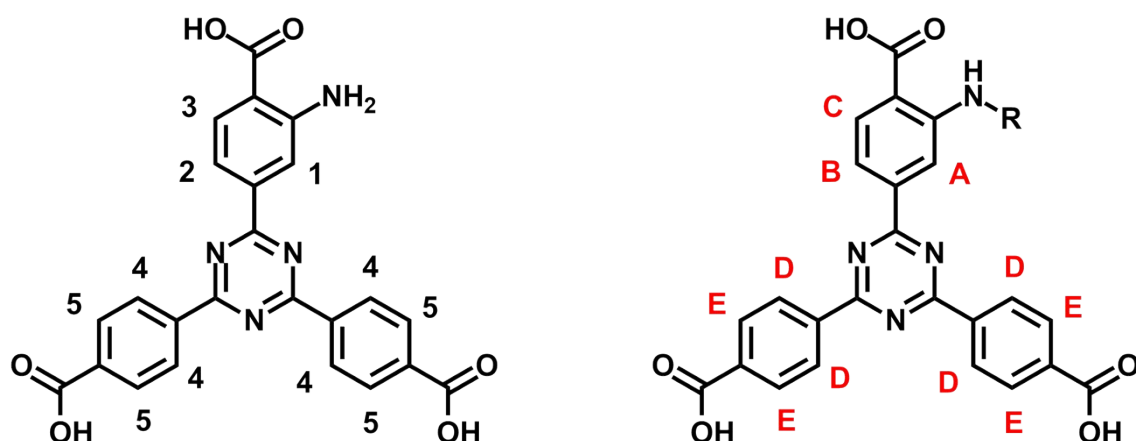
The degree of conversion after post-synthetic modification was determined by comparing the relative integrals in ¹H-NMR-spectra of digested MOFs (digested with a mixture of DMSO-d₆ and DCI (37 %)).

Table 9: Degree of conversion after post-synthetic modification of CAU-7-TATB-NH₂.

Sample	Reagent	Conversion
CAU-7-TATB-NH ₂ -AA	acetic anhydride	79 %
CAU-7-TATB-NH ₂ -VA	valeric anhydride	47 %
CAU-7-TATB-NH ₂ -SA	succinic anhydride	67 %
CAU-7-TATB-NH ₂ -PA	phthalic anhydride	35 %
CAU-7-TATB-NH ₂ -PS	1,3-propane sultone	33 %

¹H-NMR spectra

The aromatic protons of unreacted H₃TATB-NH₂ are indicated by black numbers and the protons of modified H₃TATB-NH₂ by red letters. Protons within the residue (R) are indicated in red as well. The conversion after post-synthetic modification was determined by comparing the integrals of the aromatic protons **1**, **2** or **3** with **B**. The assignments of the respective protons are shown in the following scheme:



In the following Figures only an excerpt of the ¹H-NMR spectra with significant signals is shown.

CAU-7-TATB-NH₂-AA

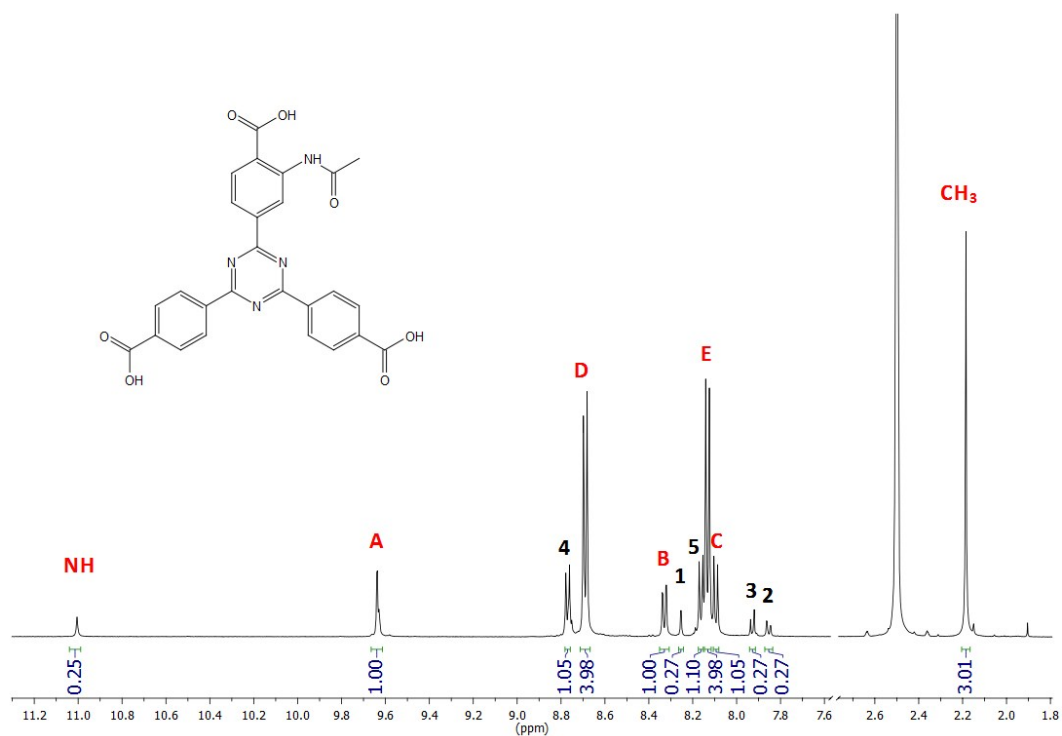


Figure S26: ¹H-NMR spectrum (500 MHz, 300 K, DMSO-d₆/DCI) of digested CAU-7-TATB-NH₂ after post-synthetic modification with acetic anhydride.

CAU-7-TATB-NH₂-VA

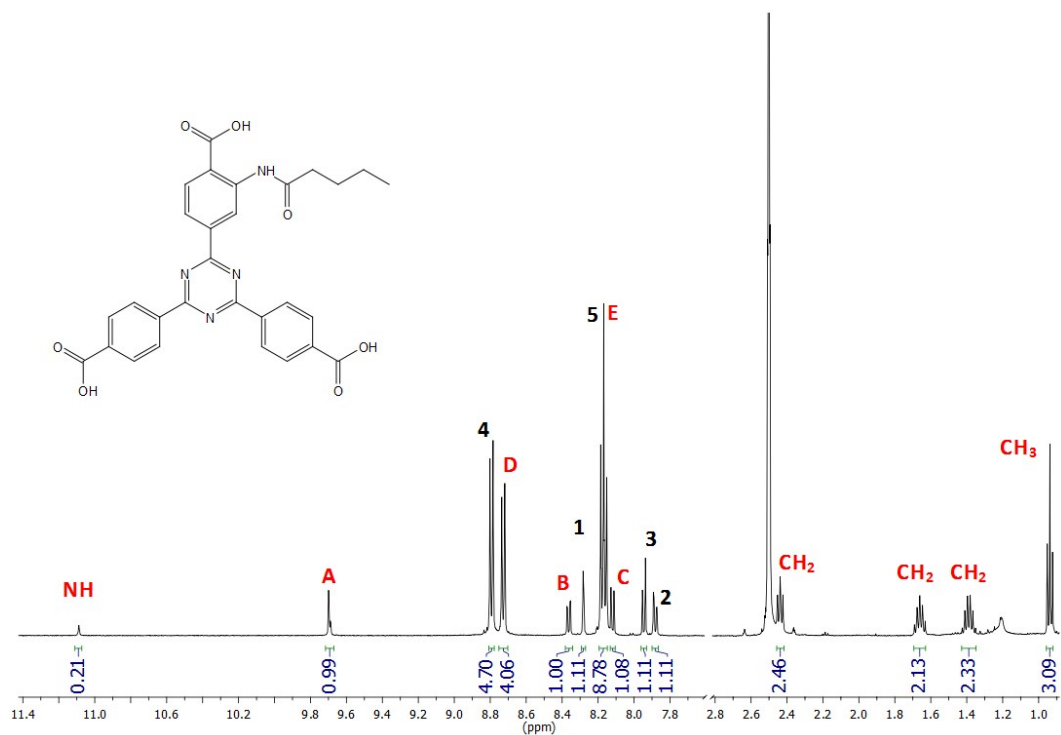


Figure S27: ¹H-NMR spectrum (500 MHz, 300 K, DMSO-d₆/DCI) of digested CAU-7-TATB-NH₂ after post-synthetic modification with valeric anhydride.

CAU-7-TATB-NH₂-SA

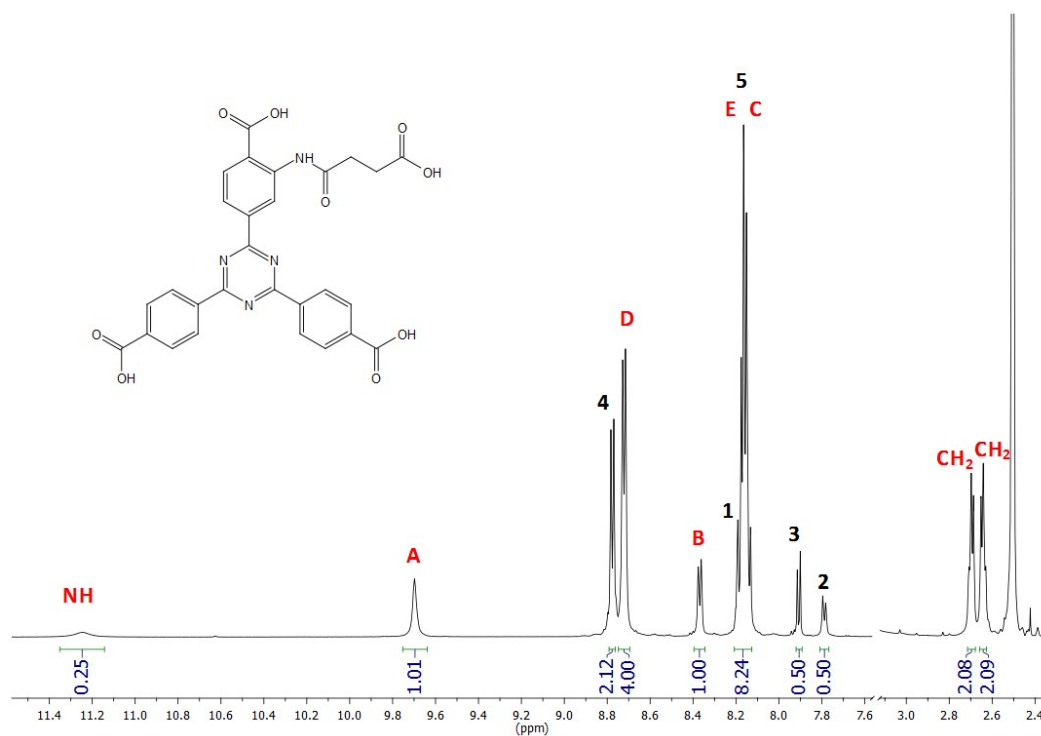


Figure S28: ¹H-NMR spectrum (500 MHz, 300 K, DMSO-d₆/DCI) of digested CAU-7-TATB-NH₂ after post-synthetic modification with succinic anhydride.

CAU-7-TATB-NH₂-PA

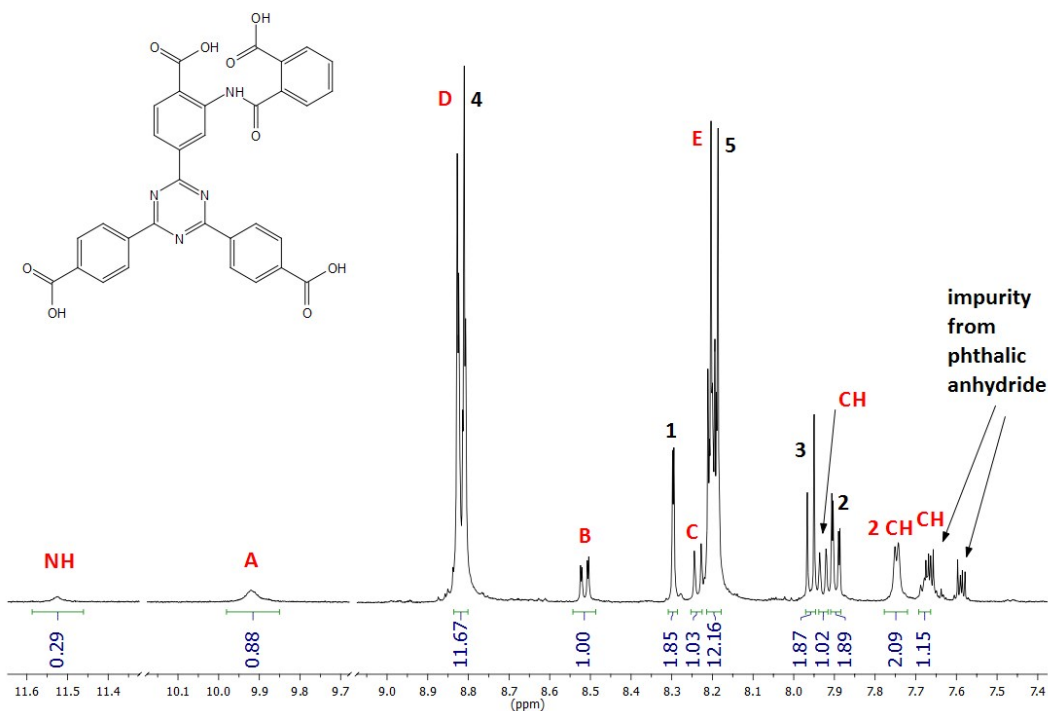


Figure S29: ¹H-NMR spectrum (500 MHz, 300 K, DMSO-d₆/DCI) of digested CAU-7-TATB-NH₂ after post-synthetic modification with phthalic anhydride.

CAU-7-TATB-NH₂-PS

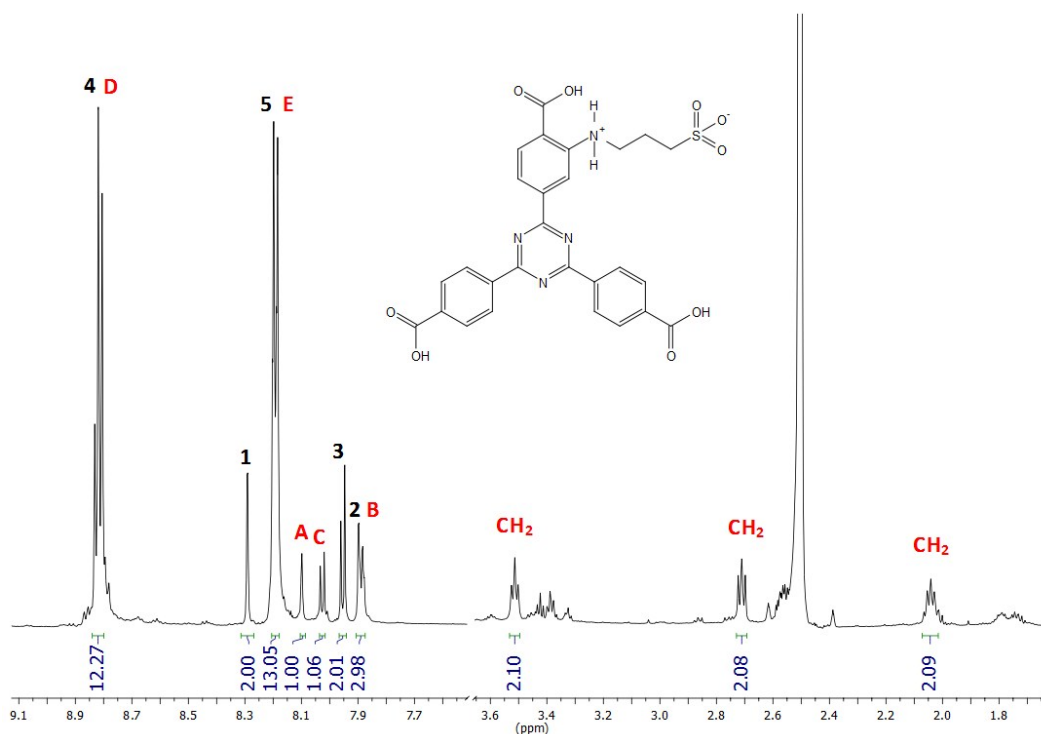


Figure S30: ¹H-NMR spectrum (500 MHz, 300 K, DMSO-d₆/DCI) of digested CAU-7-TATB-NH₂ after post-synthetic modification with 1,3-propane sultone.

Comparison of PSM with valeric anhydride for two batches with different BET surface

Despite the fact that the unmodified CAU-7-TATB-NH₂ varied in its nitrogen adsorption behaviour, the respective surface area had no influence on the degree of conversion. Two batches of CAU-7-TATB-NH₂ with different surface areas (137 m²/g and 627 m²/g) were used for a PSM with valeric anhydride. For both MOFs a similar conversion was observed (Fig. S31). This points out that the inconsistent nitrogen sorption behaviour is not influencing the porosity in fluid media.

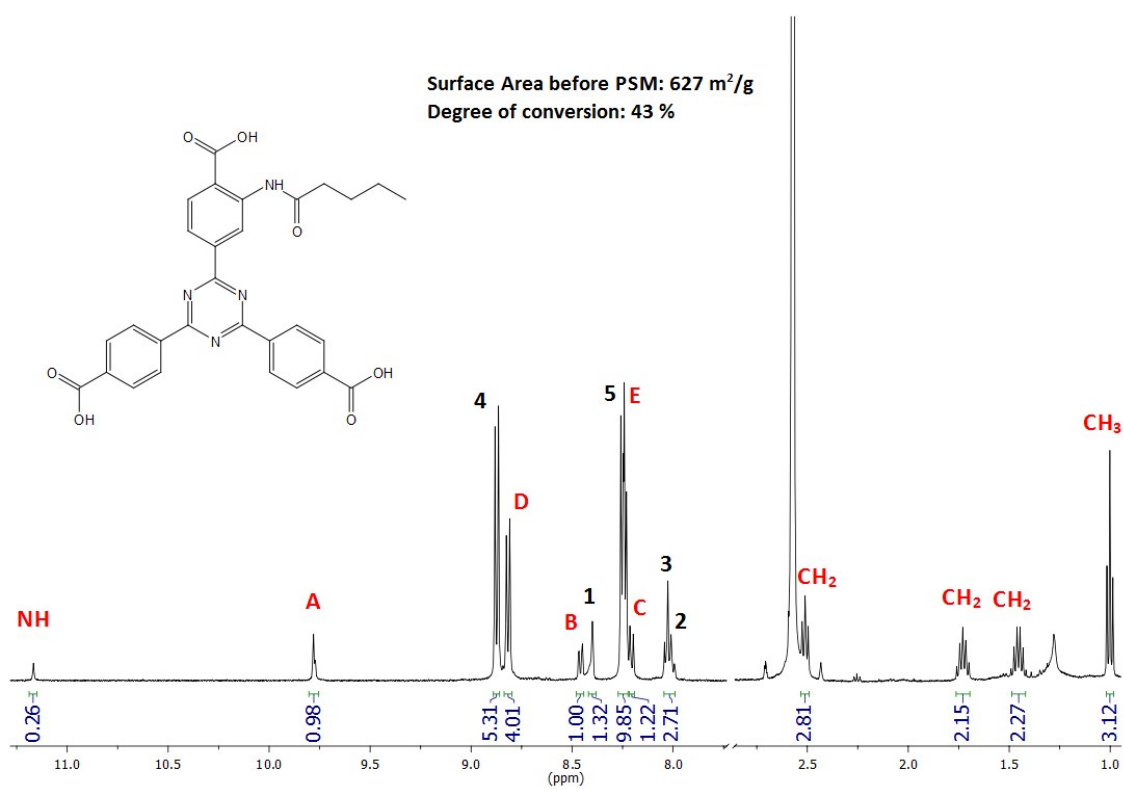
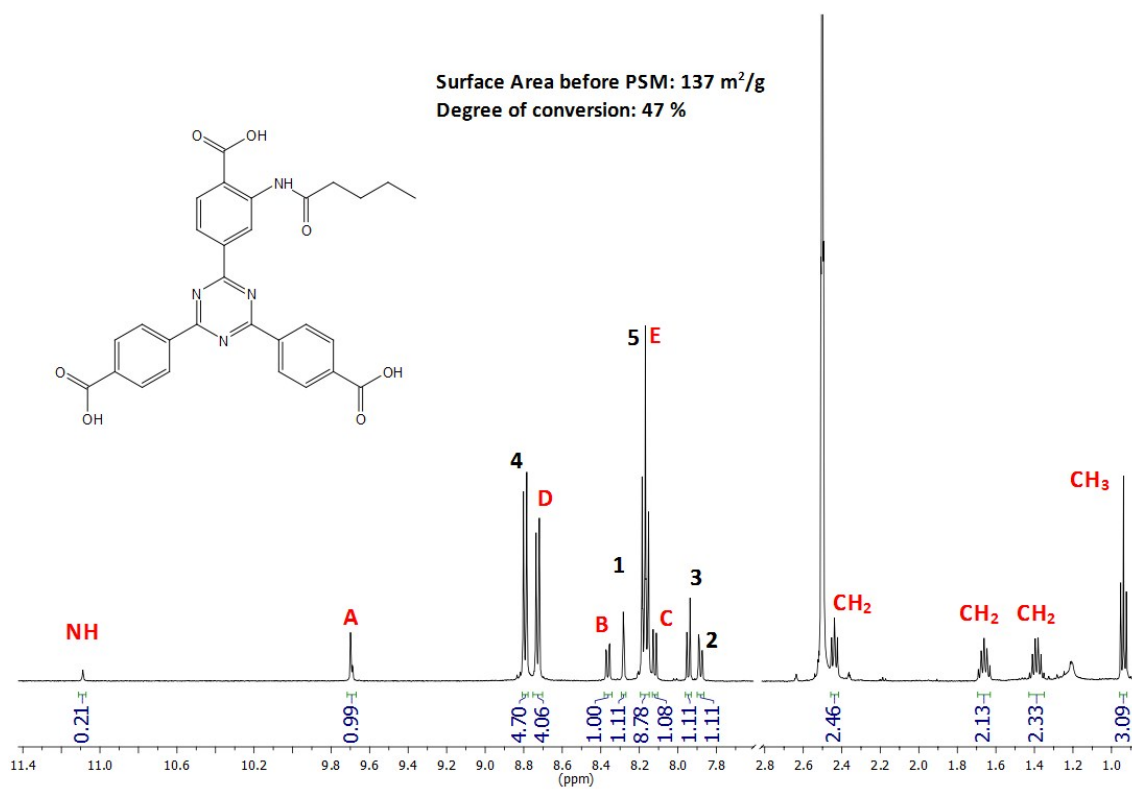


Figure S31: Comparison of ¹H-NMR spectra from PSM with valeric anhydride for two batches with different BET surface areas. The comparison of both ¹H-NMR spectra shows no significant difference in the degree of conversion.

X-ray powder diffraction

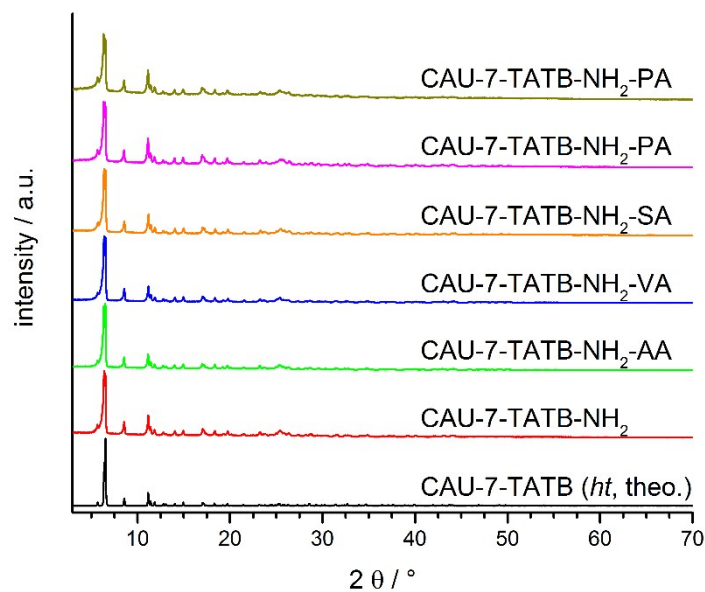


Figure S32: PXRD patterns of CAU-7-TATB-NH₂ (mixture of several batches) and the post-synthetically modified samples. For all patterns, there is no indication for loss of crystallinity due to the post-synthetic modification.

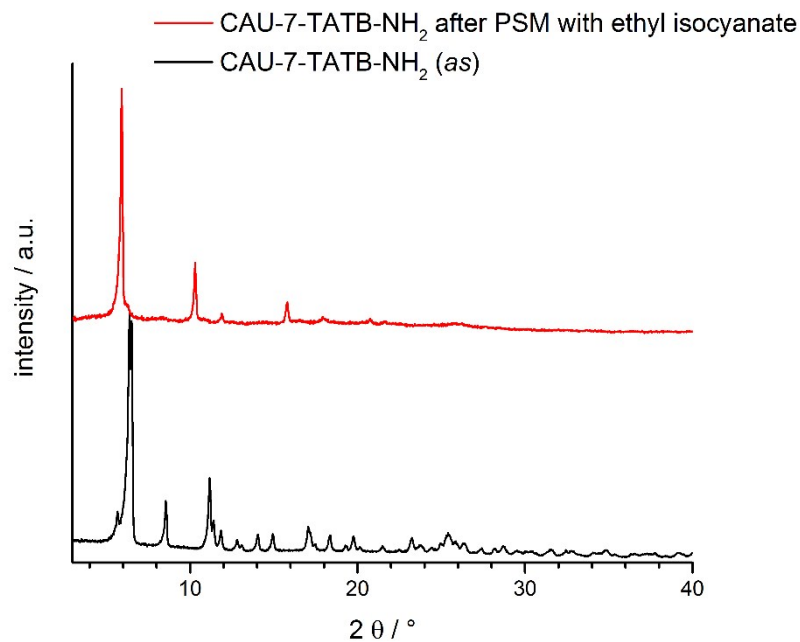


Figure S33: PXRD patterns of CAU-7-TATB-NH₂ (mixture of several batches) and the post-synthetically modified sample, which was treated with ethyl isocyanate. The reaction led to degradation of the crystal structure and formed a crystalline compound which has not identified yet.

Sorption

The N₂ sorption curves of CAU-7-TATB-NH₂ (mixture of several batches) and the post-synthetically modified samples are shown in Fig. S34. The results of the BET analysis are summarized in Table S10. It remains unclear why the post-synthetic modification reaction with acetic anhydride led to a higher specific BET surface area in the resulting product (CAU-7-TATB-NH₂-AA) when compared to the starting material CAU-7-TATB-NH₂.

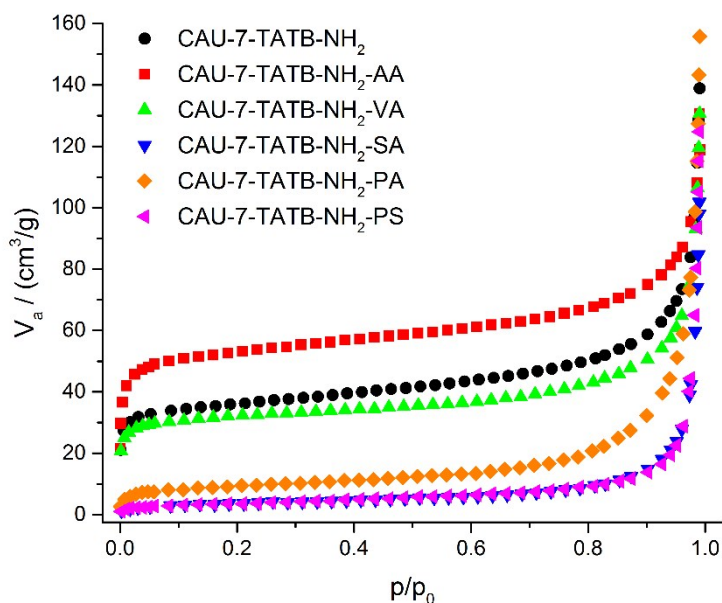


Figure S34: N₂ adsorption isotherms of CAU-7-TATB-NH₂ (mixture of several batches) and the post-synthetically modified samples, measured at 77 K. Activation of the samples at 100 °C for 12 h in vacuum. Only the adsorption curves are shown for more clarity.

Table S10: Specific BET surface areas and micropore volumes of CAU-7-TATB-NH₂ (mixture of several batches) and the post-synthetically modified samples.

Sample	A _{BET} / (m ² /g)	V _{mic} / (cm ³ /g)
CAU-7-TATB-NH ₂	137	0.06
CAU-7-TATB-NH ₂ -AA	203	0.09
CAU-7-TATB-NH ₂ -VA	123	0.05
CAU-7-TATB-NH ₂ -SA	13	0.01
CAU-7-TATB-NH ₂ -PA	33	0.02
CAU-7-TATB-NH ₂ -PS	13	0.01

Infrared spectroscopy

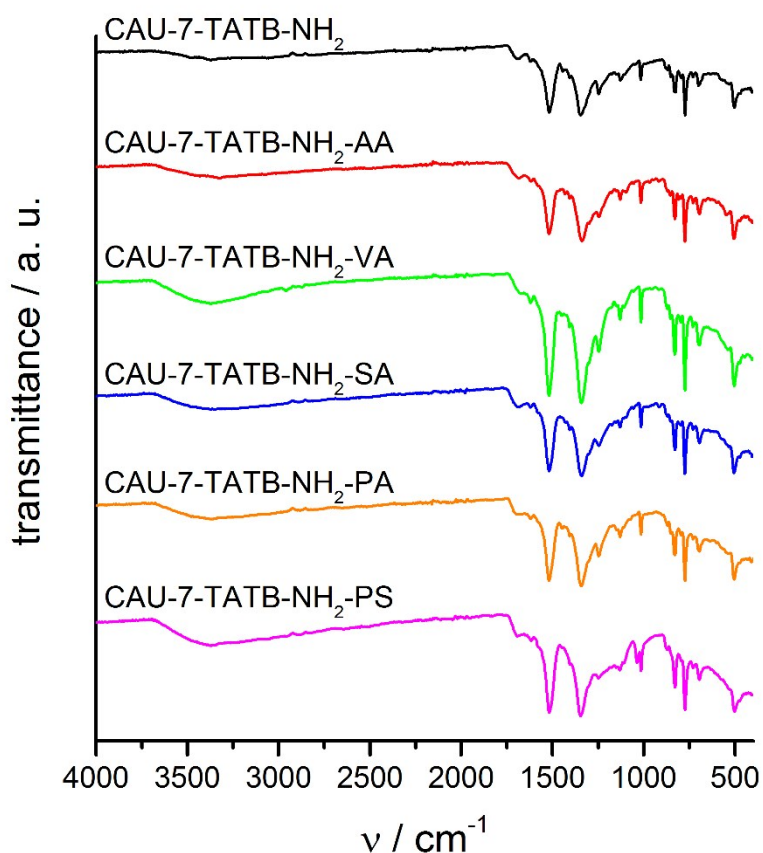


Figure S35: IR spectrum of CAU-7-TATB-NH₂ (mixture of several batches) in comparison with the spectra of the post-synthetically modified MOFs. All spectra have the same characteristic frequencies: 1518 cm⁻¹ (asymm. carboxylate), 1344 cm⁻¹ (symm. carboxylate), 829 cm⁻¹, 775 cm⁻¹ (aryl-H). The only significant difference is an additional frequency at 1036 cm⁻¹ (S=O) for CAU-7-TATB-NH₂-PS, which can be attributed to the sulfonate group.

Thermogravimetric and elemental analysis

For the analysis of CAU-7-TATB-NH₂, the same mixture of several batches was used, as it has been used for the post-synthetic modification ($A_{\text{BET}} = 137 \text{ m}^2/\text{g}$). The thermogravimetric and elemental analyses (Fig. S36, Table S11-S12) do not indicate any impurity, neither for CAU-7-TATB-NH₂, nor for the post-synthetically modified samples. The results are in agreement with the theoretical values (Table S11-S12).

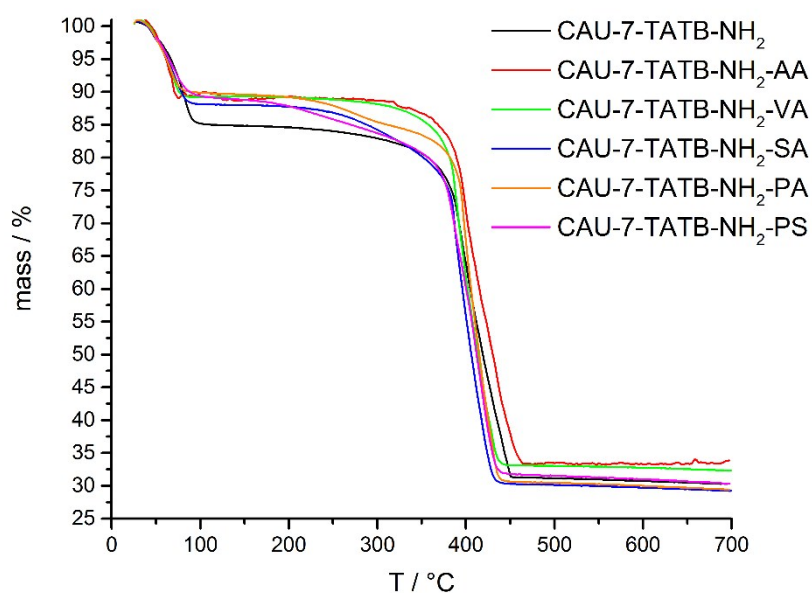


Figure S36: TG curves of CAU-7-TATB-NH₂ (mixture of several batches) and the post-synthetically modified samples.

Table S11: Combined results of the TG and elemental analysis of CAU-7-TATB-NH₂ (mixture of several batches) and the post-synthetically modified samples.

Sample		C / %	H / %	N / %	S / %	TGA 1. step / %	TGA 2. step / %
CAU-7-TATB-NH ₂	meas.	39.74	1.85	7.99	0.00	15.61	53.64
	theo.	38.82	3.39	7.99	0.00	16.05	54.42
CAU-7-TATB-NH ₂ -AA	meas.	39.55	2.04	7.27	0.00	12.38	55.31
	theo.	39.11	3.15	7.13	0.00	11.46	58.88
CAU-7-TATB-NH ₂ -VA	meas.	38.84	2.36	7.01	0.00	11.12	56.21
	theo.	39.96	3.41	7.07	0.00	11.37	59.21
CAU-7-TATB-NH ₂ -SA	meas.	38.50	2.16	6.90	0.00	12.43	57.89
	theo.	38.26	3.33	6.69	0.00	12.91	59.28
CAU-7-TATB-NH ₂ -PA	meas.	39.68	1.90	6.91	0.00	10.71	59.29
	theo.	38.45	3.23	6.97	0.00	11.20	59.83
CAU-7-TATB-NH ₂ -PS	meas.	36.73	2.51	6.79	1.66	9.44	57.39
	theo.	38.74	2.99	7.23	1.37	9.30	60.63

Table S12: Chemical formulas obtained from combined results of NMR, TG and elemental analysis of CAU-7-TATB-NH₂ (mixture of several batches) and the post-synthetically modified samples. The degree of conversion has been determined by the ¹H-NMR analyses.

Sample	Chemical formula
CAU-7-TATB-NH ₂	[Bi(TATB-NH ₂)]·5 H ₂ O·0.5 DMF
CAU-7-TATB-NH ₂ -AA	[Bi(TATB-NH ₂) _{0.21} (TATB-NHR) _{0.79}]·5 H ₂ O
CAU-7-TATB-NH ₂ -VA	[Bi(TATB-NH ₂) _{0.53} (TATB-NHR) _{0.47}]·5 H ₂ O
CAU-7-TATB-NH ₂ -SA	[Bi(TATB-NH ₂) _{0.33} (TATB-NHR) _{0.67}]·6 H ₂ O
CAU-7-TATB-NH ₂ -PA	[Bi(TATB-NH ₂) _{0.65} (TATB-NHR) _{0.35}]·5 H ₂ O
CAU-7-TATB-NH ₂ -PS	[Bi(TATB-NH ₂) _{0.67} (TATB-NHR) _{0.33}]·4 H ₂ O

References

- 1 M. Krüger, H. Reinsch, A. K. Inge and N. Stock, *Microporous Mesoporous Mater.*, 2017, **249**, 128-136.
- 2 E. Mühlbauer, A. Klinkebiel, O. Beyer, F. Auras, S. Wuttke, U. Lüning and T. Bein, *Microporous Mesoporous Mater.*, 2015, **216**, 51–55.
- 3 A. Coelho, *TOPAS Academic 4.1*, Coelho Software, 2007.
- 4 M. Feyand, E. Mugnaioli, F. Vermoortele, B. Bueken, J. M. Dieterich, T. Reimer, U. Kolb, D. de Vos and N. Stock, *Angew. Chem.*, 2012, **124**, 10519–10522, *Angew. Chem. Int. Ed.*, 2012, **51**, 10373–10376.
- 5 T. Düren, F. Millange, G. Férey, K. S. Walton and R. Q. Snurr, *J. Phys. Chem. C*, 2007, **111**, 15350–15356.
- 6 *Materials Studio 5.5.3*, Accelrys Software Inc., 2010.
- 7 V. Favre-Nicolin and R. Černý, *J. Appl. Crystallogr.*, 2002, **35**, 734–743.